

CP violation in three-body chargino decaysMakiko Nagashima,^{1,*} Ken Kiers,^{2,†} Alejandro Szykman,^{1,‡} David London,^{1,§} Jenna Hanchey,^{2,||} and Kevin Little^{2,¶}¹*Physique des Particules, Université de Montréal, C.P. 6128, succursale centre-ville, Montréal, QC, Canada H3C 3J7*²*Physics and Engineering Department, Taylor University, 236 West Reade Avenue, Upland, Indiana 46989, USA*

(Received 13 July 2009; published 10 November 2009)

CP violation in supersymmetry can give rise to rate asymmetries in the decays of supersymmetric particles. In this work we compute the rate asymmetries for the three-body chargino decays $\tilde{\chi}_2^\pm \rightarrow \tilde{\chi}_1^\pm HH$, $\tilde{\chi}_2^\pm \rightarrow \tilde{\chi}_1^\pm ZZ$, $\tilde{\chi}_2^\pm \rightarrow \tilde{\chi}_1^\pm W^+ W^-$ and $\tilde{\chi}_2^\pm \rightarrow \tilde{\chi}_1^\pm ZH$. Each of the decays contains contributions mediated by neutral Higgs bosons that can possibly go on shell. Such contributions receive a resonant enhancement; furthermore, the strong phases required for the CP asymmetries come from the widths of the exchanged Higgs bosons. Our results indicate that the rate asymmetries can be relatively large in some cases, while still respecting a number of important low-energy bounds such as those coming from B meson observables and electric dipole moments. For the parameters that we consider, rate asymmetries of order 10% are possible in some cases.

DOI: 10.1103/PhysRevD.80.095012

PACS numbers: 11.30.Pb, 11.30.Er, 14.80.Cp, 14.80.Ly

Supersymmetry (SUSY) has been proposed as a solution to the hierarchy problem in the standard model (SM). SUSY is widely thought to be the physics that lies beyond the SM, and it is hoped that it will be discovered in the future at the LHC or at a linear collider.

In SUSY theories each ordinary fermion and gauge boson has a superpartner, respectively of spin 0 and spin $\frac{1}{2}$. SUSY also includes a charged Higgs boson, the H^- . The W^- and H^- each have a fermionic partner, known as charginos. These two charginos can mix, resulting in two mass eigenstates $\tilde{\chi}_1^-$ and $\tilde{\chi}_2^-$ whose masses can be very different. Here we adopt the standard notation $m_{\tilde{\chi}_2^-} > m_{\tilde{\chi}_1^-}$. In this paper, we study CP violation in the decay $\tilde{\chi}_2^\pm \rightarrow \tilde{\chi}_1^\pm XY$, where $XY = HH, ZZ, W^+ W^-$ or ZH (H is a Higgs boson). This analysis is an extension of the work performed in Refs. [1,2]. Throughout this paper we assume that the CP-conserving SUSY parameters are known, but that those which violate CP remain to be measured. Some previous studies of CP violation involving charginos may be found in Refs. [3–11].

CP violation in SUSY has been studied extensively at low energies, in meson mixing [12], in the B -meson system [13] and in electric dipole moments (EDMs) [14]. EDMs in particular provide quite stringent constraints on the low-energy CP-violating SUSY phases of the superparticle couplings. For certain values of the SUSY parameters, there is a disagreement with the experimental limits, resulting in the so-called SUSY CP problem. In this paper we make extensive use of the computer program CPSUPERH2.0 [15–17] in choosing values for the various

SUSY parameters in our processes. The most recent version of this program allows the user to compute EDMs, as well as various other low-energy observables.

In a given decay, there are three types of CP-violating signals. First, there is the partial rate asymmetry. Any difference in the rate between process and CP-conjugate process is a signal of CP violation. As we will see, it is possible that the partial rate asymmetry is sizable (of order 5%–10% for the processes considered). Second, one has the modified (spin-dependent) rate asymmetry. Here one compares the rate for process and CP-conjugate process for the case in which the spin of one of the particles has been measured. This measurement is complicated, and so, given that the partial rate asymmetry can be significant, we do not consider the modified rate asymmetry in this paper. The third CP-violating signal is the triple-product (TP) asymmetry, which is proportional to $\vec{v}_1 \cdot (\vec{v}_2 \times \vec{v}_3)$ (each v_i is a spin or momentum). This is due to terms of the form $\text{Tr}[\gamma_\alpha \gamma_\beta \gamma_\rho \gamma_\sigma \gamma_5]$ in the square of the amplitude. Since only three-body decays are considered here, a nonzero TP can arise only if a spin or polarization is measured. As noted above, such measurements are difficult, and so we do not consider TPs here. Thus, the only CP-violating signal analyzed in this paper is the partial rate asymmetry.

All effects that violate CP require the interference of (at least) two amplitudes. The partial rate asymmetry is proportional to $\sin\delta$, where δ is the relative strong (CP-even) phase between the interfering amplitudes. Strong phases can be generated in one of two ways. First, one can have the exchange of gluons between the particles involved in the decay, leading to QCD-based strong phases. Unfortunately, we do not know how to calculate the strong phases in this case. Alternatively, the strong phases can be generated by the (known) widths of the intermediate particles in the decay. In the decays considered in this paper, the particles do not couple to gluons. Thus, the strong phase arises only due to the widths of the intermediate

*makiko@LPS.umontreal.ca

†knkiers@taylor.edu

‡szykman@lps.umontreal.ca

§london@lps.umontreal.ca

||jenna.hanchey@gmail.com

¶little@uchicago.edu

particles. This is good, given that we want to *measure* the CP violation, and not simply detect its presence.

Now, SUSY includes two Higgs doublets which contain (in the gauge basis) two neutral scalars and one pseudo-scalar. In the mass basis, these particles mix and one obtains three mass eigenstates H_1 , H_2 and H_3 . In SUSY theories, the lightest mass is $m_{H_1} = O(100)$ GeV and we therefore take the final-state H to be H_1 .

Figure 1 shows the diagrams that contribute to $\tilde{\chi}_2^- \rightarrow \tilde{\chi}_1^- H_1 H_1$. The diagrams for the ZZ case are identical, but with H_1 replaced by Z in the final state. The WW diagrams are similar, except that there is no diagram analogous to Fig. 1(b) (we take “ p_4 ” to correspond to the W^- for this decay). Furthermore, the diagram analogous to Fig. 1(c) involves intermediate neutralinos instead of charginos, and there is an extra diagram similar to Fig. 1(a), but with the intermediate Higgs bosons replaced by the Z . Finally, for the ZH_1 case the diagrams are similar to Fig. 1, but with one H_1 replaced by Z . Also, there is an extra diagram similar to Fig. 1(a), but with the intermediate Higgs bosons replaced by the Z . Note that the neutralinos, $\tilde{\chi}_i^0$ ($i = 1, \dots, 4$), are the fermionic partners of the γ , Z , and neutral Higgs bosons.

The decay amplitudes that are of most interest to us arise from diagrams containing an intermediate particle that can go on shell. Such diagrams can benefit from a resonant enhancement. The internal $\tilde{\chi}_{1,2}^-$, H_1 and Z can never be on shell, while the H_2 and H_3 can be. (For a given set of SUSY parameters, the widths Γ_2 and Γ_3 are calculable, as are the “off-diagonal widths” associated with transitions $H_i \leftrightarrow H_j$ [18]. These terms are taken into account by CPSUPERH2.0 when it computes the neutral Higgs propagator matrix.) The case of internal neutralinos (which appear in the case $XY = W^+ W^-$) is more complicated. In principle, these could be on shell. Unfortunately, we do not know their widths, making their contributions to the rate asymmetry uncertain. In practice, for the cases that we consider, the two heavier neutralinos have masses close to $m_{\tilde{\chi}_2^-}$ and the two lighter neutralinos have masses close to or less than $m_{\tilde{\chi}_1^-}$. Thus, in the examples we consider, the neutralinos cannot go on shell and the uncertainty associated with the neutralinos’ (unknown) widths is mitigated.

In order for a given partial rate asymmetry to be appreciable, the interfering amplitudes should be of comparable sizes. Furthermore, since the rate asymmetries depend on an integration over phase space, the “large” contributions from these amplitudes should occur in similar regions of phase space. This latter requirement is met if the masses of the on-shell particles, H_2 and H_3 , are similar. Fortunately, it is relatively common in SUSY theories that $m_{H_2} \approx m_{H_3}$ [19]. The decay amplitudes of most interest to us, therefore, are those dominated by internal H_2 and H_3 exchange. In calculating the square of the amplitude, however, we retain the contributions of various nonresonant diagrams (see Fig. 1), since they can in principle give non-negligible

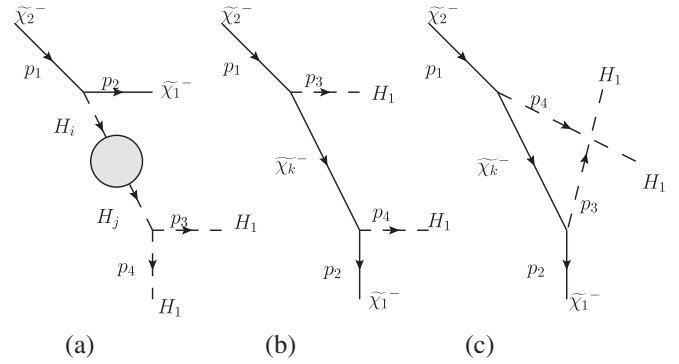


FIG. 1. Feynman diagrams for the decay $\tilde{\chi}_2^- \rightarrow \tilde{\chi}_1^- H_1 H_1$. In diagram (a) the decay is mediated by neutral Higgs bosons, while diagrams (b) and (c) are mediated by charginos.

contributions. With these ingredients, we calculate the partial rate asymmetry. Since it is assumed that the masses are known, we can determine whether or not CP violation is likely in these decays. Measurement of these CP asymmetries will allow experimentalists to extract and/or constrain the SUSY parameters, including CP -violating SUSY phases.

Analytical expressions for the amplitudes in question may be found in the appendix. Our notation is similar or identical to that employed in Ref. [15]. We have also used Feynman rules derived from Refs. [20,21] where necessary. FEYNCALC [22] was used to compute the squares of the amplitudes. The resulting expressions are quite messy and have not been included here. Please also note the following:

- (1) Although only H_2 and H_3 can go on shell,¹ we have allowed for the possibility of nonzero widths for other intermediate particles. For the purpose of our numerical work, all non-Higgs intermediate particles (with the exception of the Z , whose width is known) have been given a uniform width of 10 GeV. Since the intermediate particles in question are off shell, the quantities that we compute should not be very sensitive to the value(s) assumed for the intermediate particles’ widths. We have explicitly checked the effect of changing the uniform width from 10 GeV to 1 GeV and to 20 GeV for the data points plotted in Figs. 2 and 3 and have confirmed that the quantities shown in these plots are not very sensitive to such changes.
- (2) The inclusion of intermediate particles’ widths in our calculation implies that certain beyond-tree-level diagrams have effectively been taken into account. Other such diagrams have not been included, leading to possible issues with gauge dependence or with respect to the CP - CPT connection [23,24].

¹As noted above, the neutralinos can in principle go on shell in the “ WW ” case, but they do not do so for the parameters that we use.

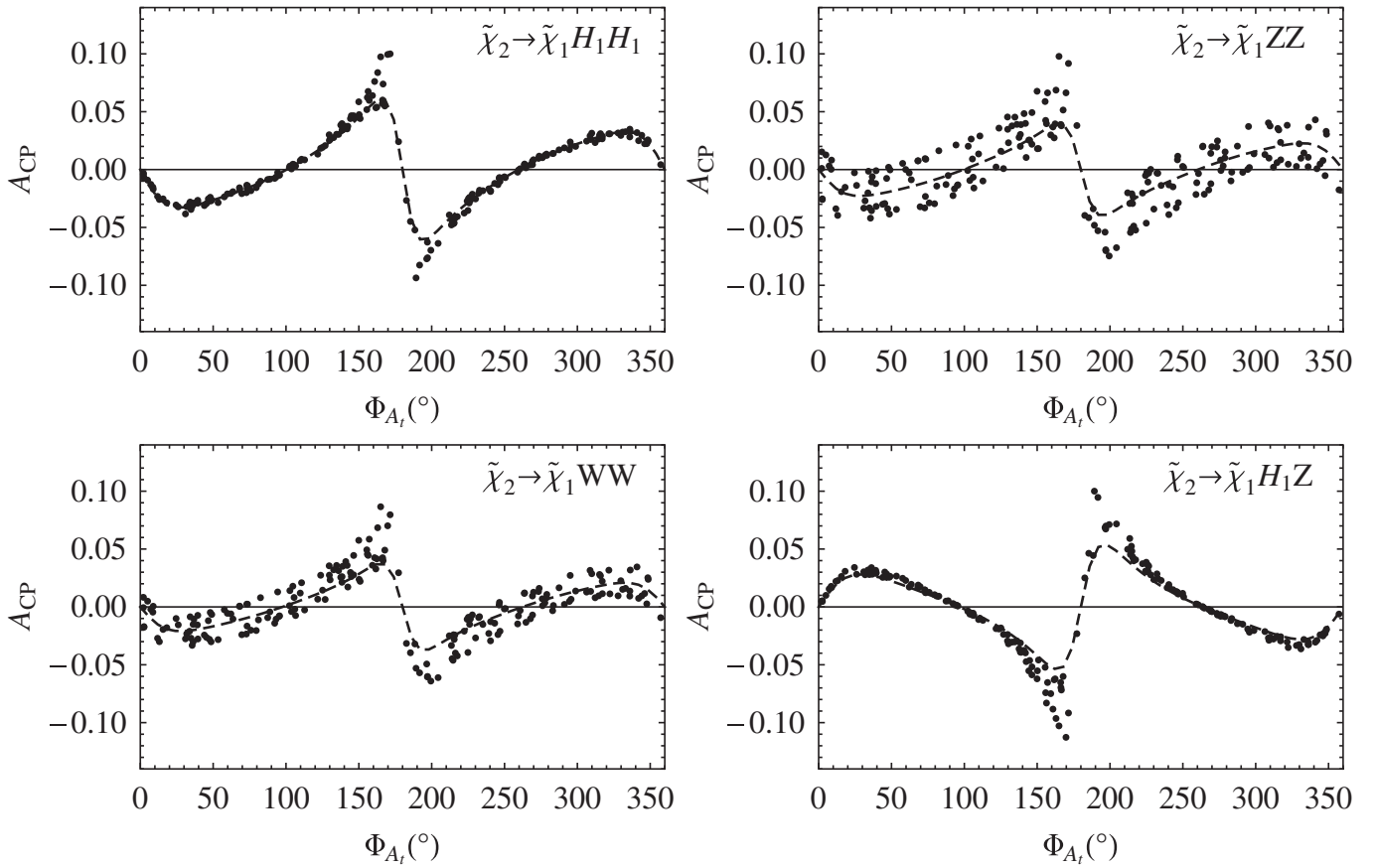


FIG. 2. Plots of partial rate asymmetries as a function of Φ_{A_τ} . The dashed lines show the asymmetries for the case $\Phi_1 = \Phi_2 = \Phi_3 = \Phi_{A_b} = \Phi_{A_\tau} = 0^\circ$ (the values of the other SUSY parameters are given in the text). The scattered points indicate the asymmetries obtained by allowing all six phases to vary randomly between 0° and 360° . Low-energy experimental results have not been used to constrain the SUSY parameter space when generating these plots.

CPSUPERH2.0 uses the Pinch technique when computing the elements of the neutral Higgs propagator matrix [25,26]. This technique was designed in such a way that certain classes of diagrams would be gauge independent. The neutral Higgs propagator matrix is a 4×4 matrix in this approach rather than the 3×3 matrix that one might expect. Rigorous application of the Pinch technique for the present calculation is beyond the scope of our paper. Instead, we have used the 3×3 physical Higgs block of the 4×4 propagator computed by CPSUPERH2.0 and have used Feynman rules consistent with the unitary gauge.

- (3) It is understood that H_1 is not, in general, a CP eigenstate, since the scalar and pseudoscalar Higgs bosons can mix when CP is violated. Nevertheless, we have checked numerically that the asymmetries for the $H_1 H_1$ and $Z H_1$ case are in fact zero when all CP -violating phases are zero.

Having used the expressions in the appendix to compute the widths for the processes and CP -conjugate processes, we subtract one from the other to obtain the respective partial rate asymmetries,

$$\mathcal{A}_{CP}^{XY} \equiv \frac{\Gamma(\tilde{\chi}_2^- \rightarrow \tilde{\chi}_1^- XY) - \Gamma(\tilde{\chi}_2^+ \rightarrow \tilde{\chi}_1^+ XY)}{\Gamma(\tilde{\chi}_2^- \rightarrow \tilde{\chi}_1^- XY) + \Gamma(\tilde{\chi}_2^+ \rightarrow \tilde{\chi}_1^+ XY)}, \quad (1)$$

with $XY = H_1 H_1, ZZ, W^+ W^-$ or $Z H_1$.

The SUSY parameter space to be considered is enormous, and we have not made any attempt to perform a systematic parameter scan in our numerical work. Rather, we have chosen to focus on a small region of parameter space that is of interest. In particular, we have focused on a variation of the ‘‘CPX’’ scenario described in Ref. [17]. In the CPX scenario, the SUSY parameters μ, A_t, A_b and A_τ are chosen in such a way that $|\mu A_{t,b,\tau}| = 8M_{\text{SUSY}}^2$, where M_{SUSY} represents the common mass scale of the third-generation squarks and sleptons (see Refs. [17,27] for further details), and $A_{t,b,\tau}$ are trilinear couplings in the soft SUSY-breaking Lagrangian. This scenario was originally motivated by the observation that certain CP -violating terms in the neutral Higgs mass-squared matrix depend on $\text{Im}(\mu A_t)/M_{\text{SUSY}}^2$. In our variation on the CPX scenario, we set $|\mu| = 0.6 \text{ TeV}$ and $M_{\tilde{Q}_3} = M_{\tilde{U}_3} = M_{\tilde{D}_3} = M_{\tilde{L}_3} = M_{\tilde{E}_3} = M_{\text{SUSY}} = 0.5 \text{ TeV}$, as well as $|M_2| = 2|M_1| = 200 \text{ GeV}$, $|M_3| = 1 \text{ TeV}$,

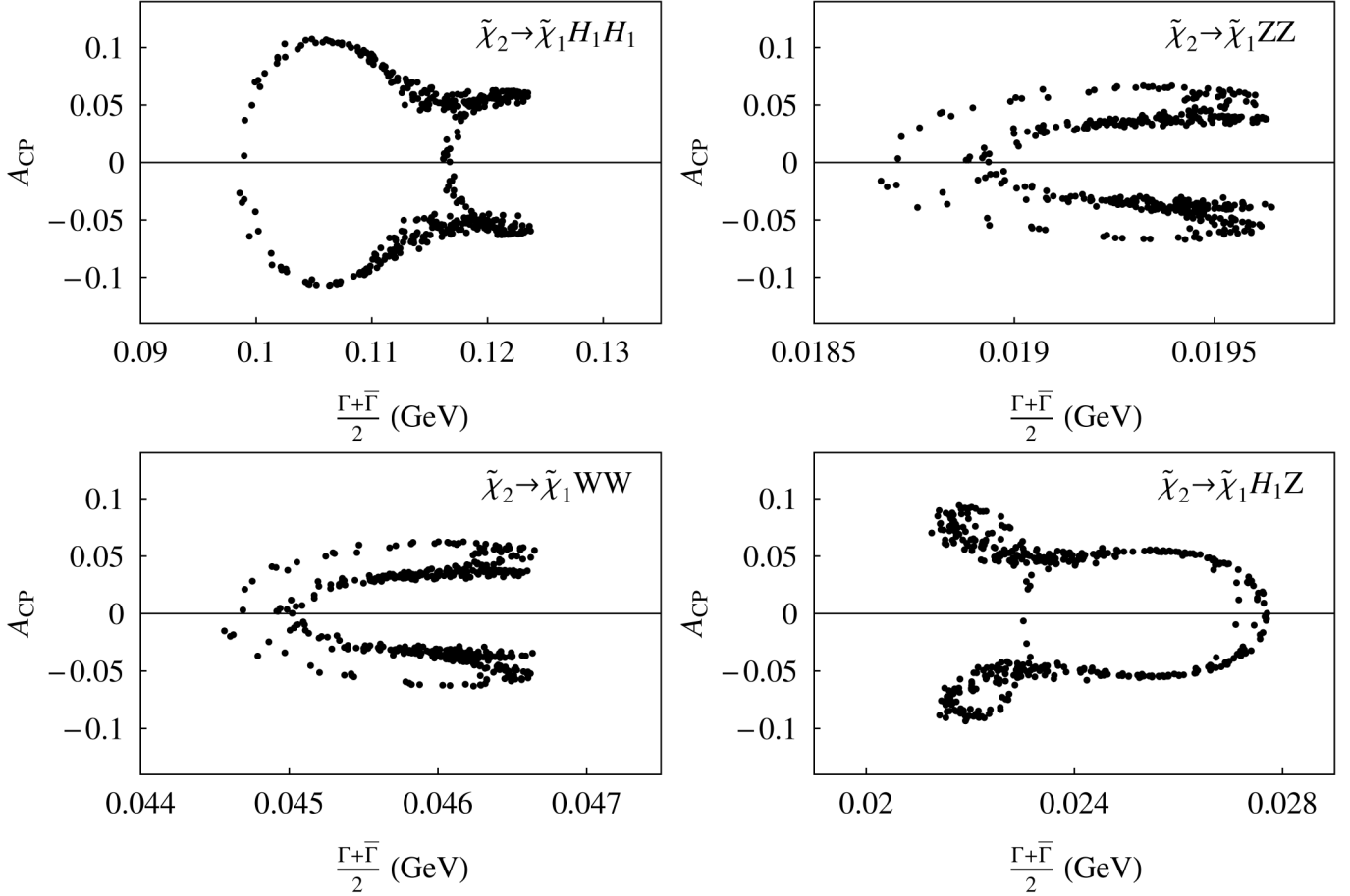


FIG. 3. Scatter plots of partial rate asymmetries versus mean widths for $\tilde{\chi}_2 \rightarrow \tilde{\chi}_1 XY$, with $XY = H_1 H_1, ZZ, W^+ W^-$ or $Z H_1$.

$m_{H^\pm} = 300$ GeV and $\tan\beta = 5$. Also, we set $|A_{u,d,c,s,e,\mu}| = |A_{t,b,\tau}| = 1$ TeV and $\Phi_{A_{u,d,c,s,e,\mu}} = 0^\circ$. Our notation here is the same as that used in Ref. [17].

Figure 2 shows the four asymmetries under consideration, plotted as functions of Φ_{A_t} . For the purpose of the plots, the hierarchy factors ρ_J ($J = Q, U, D, L, E$) have all been set to 10.² The dashed line in each plot shows the result obtained by allowing Φ_{A_t} to vary between 0° and 360° , while keeping the other five phases set to zero. (That is, we set $\Phi_1 = \Phi_2 = \Phi_3 = \Phi_{A_b} = \Phi_{A_\tau} = 0^\circ$, where $\Phi_{1,2,3}$ are the phases associated with the complex gaugino mass parameters $M_{1,2,3}$. Note that throughout this work we adopt the convention that $\Phi_\mu = 0^\circ$.) The scattered points in these plots show the asymmetries obtained by allowing all six phases to vary randomly between 0° and 360° . As is evident from the figure, for the parameters we have chosen,

²In the notation of CPSUPERH2.0, the mass parameters M_{J_1} and M_{J_2} are assumed to be equal to each other (here $J = Q, U, D, L, E$ and the subscripts “1” and “2” refer to the first and second generation, respectively). The third-generation mass parameters are allowed to be different from those of the first two. The hierarchy factors are defined via the following expression: $M_{J_{12}} = \rho_J M_{J_3}$.

the asymmetries are strongly dependent on Φ_{A_t} , although other phases contribute to the asymmetries as well. Analogous plots, showing the asymmetries as functions of the other five phases, do not demonstrate the same pronounced dependence on the other phases.

In generating the data for Fig. 2 we have not made any attempt to impose the various low-energy experimental constraints that are available, since the purpose of the plots is to demonstrate the functional dependence of the asymmetries on the phases. We now turn to a more careful consideration of the asymmetries by also taking into account several low-energy constraints.

The constraints we impose are listed in Table I, which also contains some comments regarding the constraints. We offer here a few additional comments. Let us first consider the muon anomalous magnetic moment. According to the authors of Ref. [33], the experimental value for the muon anomalous magnetic moment exceeds the SM prediction by $\Delta a_\mu = a_\mu^{\text{exp}} - a_\mu^{\text{SM}} = (30.7 \pm 8.2) \times 10^{-10}$, which represents a 3.7σ deviation. One option would be to require that the SUSY contribution make up the difference between the experimental value and the SM prediction. We take a somewhat broader view and require the SUSY contribution to be between zero and

TABLE I. Constraints imposed when choosing SUSY parameter values for Figs. 3 and 4. The first five rows refer to the EDMs for thallium, the electron, mercury, the neutron and the muon, respectively; the sixth row contains the bound we enforce for the SUSY contribution to the muon anomalous magnetic dipole moment. Further discussion of some of the constraints may be found in the text. Note the following: (1) there is some variation in the confidence levels corresponding to the experimental upper bounds quoted in the second column; (2) Refs. [17,28] contain further information regarding the thallium EDM; and (3) to obtain the bound for the $B \rightarrow X_s \gamma$ branching ratio we have combined errors in quadrature to obtain $(3.52 \pm 0.25) \times 10^{-4}$ and have doubled the uncertainty. The range quoted in the table, and the constraint imposed, is thus at approximately the 2σ level.

Quantity	Constraint imposed	References
$ d_{\text{Tl}} $	$< 9 \times 10^{-25} e \text{ cm}$	[17,28,29]
$ d_e $	$< 1.6 \times 10^{-27} e \text{ cm}$	[29]
$ d_{199\text{Hg}} $	$< 3.1 \times 10^{-29} e \text{ cm}$	[30]
$ d_n $	$< 2.9 \times 10^{-26} e \text{ cm}$	[31]
$ d_\mu $	$< 1.8 \times 10^{-19} e \text{ cm}$	[32]
a_μ^{SUSY}	$(19.45 \pm 19.45) \times 10^{-10}$	[33]
$\mathcal{B}(B \rightarrow X_s \gamma)$	$(3.52 \pm 0.50) \times 10^{-4}$	[34]
$\mathcal{A}_{CP}(B \rightarrow X_s \gamma)$	-0.012 ± 0.028	[34]
$\mathcal{B}(B_s \rightarrow \mu^+ \mu^-)$	$< 4.7 \times 10^{-8}$	[35]
$\mathcal{B}(B_d \rightarrow \tau^+ \tau^-)$	$< 4.1 \times 10^{-3}$	[35]
$ \Delta M_{B_d}^{\text{SUSY}} $	$< 0.005 \text{ ps}^{-1}$	[35]
$ \Delta M_{B_s}^{\text{SUSY}} $	$< 0.12 \text{ ps}^{-1}$	[35]

$(30.7 + 8.2) \times 10^{-10} = 38.9 \times 10^{-10}$. The constraint quoted in Table I is thus $a_\mu^{\text{SUSY}} = (19.45 \pm 19.45) \times 10^{-10}$. The last two rows of the table describe constraints on the SUSY contributions to ΔM_{B_d} and ΔM_{B_s} . The experimental values for these quantities are $\Delta M_{B_d} = 0.507 \pm 0.005 \text{ ps}^{-1}$ and $\Delta M_{B_s} = 17.77 \pm 0.12 \text{ ps}^{-1}$ [35]. The corresponding constraints that we have listed are thus just the experimental uncertainties in these quantities. These constraints are tighter than they need to be, since we are ignoring the theoretical uncertainties within the SM. Nevertheless, these particular constraints are easily passed for the parameters we consider. One constraint that we have not directly imposed is on the ratio $R_{B\tau\nu} \equiv \mathcal{B}(B^- \rightarrow \tau^- \bar{\nu})/\mathcal{B}^{\text{SM}}(B^- \rightarrow \tau^- \bar{\nu})$. There has been some discussion in the literature regarding the possible range of this ratio. For the parameters used to generate Fig. 3 (see below), we find $R_{B\tau\nu} \sim 0.985$, which is easily within the range derived, for example, in Ref. [36].

Figure 3 shows the four asymmetries plotted as functions of the mean width [defined to be $[\Gamma(\tilde{\chi}_2^- \rightarrow \tilde{\chi}_1^- XY) + \Gamma(\tilde{\chi}_2^+ \rightarrow \tilde{\chi}_1^+ XY)]/2$, with $XY = H_1 H_1, ZZ, W^+ W^-$ or ZH_1]. The SUSY parameter values or ranges used to generate the plots in Fig. 3 are the same as those used to generate the scattered points in Fig. 2, but with three changes. First, instead of fixing the ρ_J ($J = Q, U, D,$

L, E) to a particular value, as was done for Fig. 2, we have now allowed the five hierarchy parameters to vary independently (and randomly) in the range 8 to 12. Second, we have imposed the constraints described in Table I. (The quantities in the table are computed automatically by the CPSUPERH2.0 software.) Imposing the constraints from Table I leads to relatively strong limits on the SUSY parameter space. This led us to make a third change: to increase the efficiency of our numerical work, we allowed Φ_2 only to take on the values 0° and 180° , and we restricted Φ_{A_i} so that it took on values between 140° and 220° . Of the 10^4 parameter sets that were originally generated in this manner, 432 were able to pass all of the cuts. The 432 parameter sets did not contain any cases in which Φ_2 was 180° (i.e., only the parameter sets with $\Phi_2 = 0^\circ$ survived the cuts). Parameter sets that passed all of the constraints were used to compute the widths and asymmetries that appear in Fig. 3.³ For the sets of parameters considered, and respecting various low-energy bounds, asymmetries of order 10% are possible for $\tilde{\chi}_2 \rightarrow \tilde{\chi}_1 H_1 H_1$ and slightly smaller asymmetries occur for the other decay modes.

With the parameters used for the plots in Fig. 3, the three neutral Higgs bosons had masses $m_{H_1} \sim 112.9$ – 119.5 GeV , $m_{H_2} \sim 289.3$ – 290.3 GeV and $m_{H_3} \sim 291.1$ – 292.1 GeV . Also, the lighter and heavier charginos had masses $m_{\tilde{\chi}_1} \sim 191.6 \text{ GeV}$ and $m_{\tilde{\chi}_2} \sim 613.3 \text{ GeV}$, respectively. Thus, the parameters were such that the two heavier Higgs bosons could go on shell when mediating the various decay processes, as was noted above.

Figure 4 shows the correlations between Φ_3 and Φ_{A_i} for the parameter sets that passed the constraints from Table I and that were subsequently used for the plots in Fig. 3. As is evident from the figure, there is a strong correlation between these two phases that comes into play in allowing the constraints to be passed.

It is useful to consider the observability of a 10% partial rate asymmetry. After considering the main contributions from the open two-body decay channels, we estimate the total width of the heavier chargino to be of order 10–20 GeV within the allowed parameter space region. This result, together with the $\tilde{\chi}_2 \rightarrow \tilde{\chi}_1 H_1 H_1$ partial width, allows us to obtain a representative value for the statistical significance of the CP asymmetry, $S \sim |A_{CP}|/\sqrt{2N}$, where N is the number of events corresponding to the decay under study. (N represents the number of $\tilde{\chi}_2^+$ events, as well as

³A few technical notes regarding our calculation are the following: (i) CPSUPERH2.0 follows three separate approaches when computing the neutron EDM and thus gives three separate estimates for the EDM [17]. In our numerical work, we insisted that at least one of these three numbers satisfy the neutron EDM constraint listed in Table I. (ii) We used the (approximate) default method for dealing with the dimension-six Weinberg operator, rather than supplying our own integration routine. See Ref. [17] for further discussion.

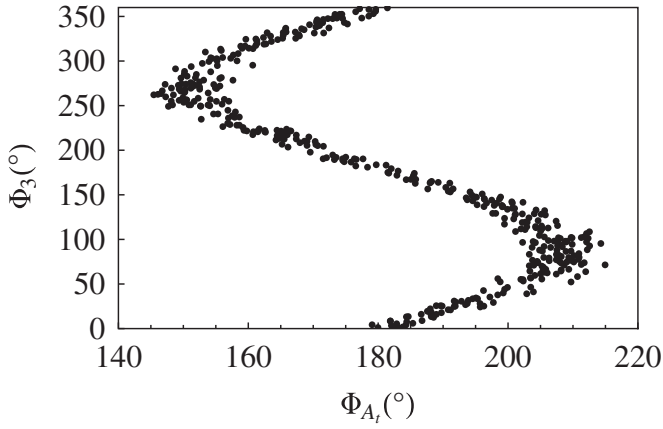


FIG. 4. Correlations between Φ_3 and Φ_{A_i} . The points shown correspond to the same parameters used to generate Fig. 3.

the number of $\tilde{\chi}_2^-$ events; these are assumed to be similar.) If, for example, the partial rate asymmetries are measured at an e^+e^- linear collider, with a single $\tilde{\chi}_2$ production cross section of order 20 fb and an integrated luminosity of $\mathcal{L} = 500 \text{ fb}^{-1}$ [4,5], then the statistical significance turns out to be of order unity. This value should be understood as a very crude estimate, since the $\tilde{\chi}_2$ production cross section is strongly dependent on the SUSY parameters and since we have not performed a detailed analysis, nor considered the case of the LHC. Our point is simply to show that a 10% partial rate asymmetry could well be reachable.

In conclusion, if SUSY is discovered in future experiments, it will become important to measure the underlying parameters of the theory. This paper has examined four chargino decay modes that could help provide insight into the CP nature of the theory. In particular, we have computed partial rate asymmetries for the decays $\tilde{\chi}_2^\pm \rightarrow \tilde{\chi}_1^\pm H_1 H_1$, $\tilde{\chi}_2^\pm \rightarrow \tilde{\chi}_1^\pm ZZ$, $\tilde{\chi}_2^\pm \rightarrow \tilde{\chi}_1^\pm W^+ W^-$ and $\tilde{\chi}_2^\pm \rightarrow \tilde{\chi}_1^\pm ZH_1$. Rate asymmetries have an advantage over some other CP -violating observables in that no spins or polarizations need to be measured. In the numerical example that we studied, it was found that the rate asymmetries for these decay modes are particularly sensitive to the phase of A_i , although other phases contribute to the asymmetries as well. For the parameters considered, asymmetries of order 10% were found for $\tilde{\chi}_2^\pm \rightarrow \tilde{\chi}_1^\pm H_1 H_1$; somewhat smaller asymmetries were found for the other decay modes. Should SUSY be discovered, chargino decays could provide a useful avenue for investigating the CP structure of the theory.

We would like to thank J. S. Lee for helpful correspondence. This work was financially supported by NSERC of Canada. The work of J. H., K. K. and K. L. was supported in part by the U.S. National Science Foundation under Grant No. PHY-0601103; K. K. was also supported in part by the U.S. National Science Foundation under Grant No. PHY-0900914.

APPENDIX: EXPRESSIONS FOR THE DECAY AMPLITUDES OF $\tilde{\chi}_2^\pm \rightarrow \tilde{\chi}_1^\pm XY$

This appendix contains analytical expressions for the amplitudes associated with the processes considered in this paper.

Let us first clarify our notation for the various propagators. We define Breit-Wigner-type propagators for chargino and neutralino internal lines as follows,

$$i(\not{p} + m)\tilde{D}(p^2, m^2, \Gamma) \equiv \frac{i(\not{p} + m)}{p^2 - m^2 + i\Gamma m} \quad (\text{A1})$$

where the tilde is used to distinguish the Breit-Wigner propagators from the 3×3 Higgs propagator D_{ij} to be described below. We also employ the Breit-Wigner form of the propagator for the graphs mediated by a Z boson. The Z propagator in the unitary gauge is $i\tilde{D}(p_Z^2, m_Z^2, \Gamma_Z)(-g^{\alpha\beta} + p_Z^\alpha p_Z^\beta / m_Z^2)$.⁴

As noted in the text, our calculation employs the 3×3 physical Higgs boson block of the full 4×4 neutral Higgs propagator computed by CPSUPERH2.0. We also differ notationally from CPSUPERH2.0 in terms of the overall normalization of the propagator. The specific relationship between the two sets of notation (within the physical 3×3 block) is the following,

$$D_{ij}(M^2) = D_{ij}^{\text{CPSUPERH}}(M^2)/M^2. \quad (\text{A2})$$

Unless noted otherwise, our notation for coupling constants and diagonalization matrices follows the notation used in Ref. [15]. One exception is the definition of $g_{H_i H_j Z}$ (which occurs in the “ ZH_1 ” decay), for which we use the notation defined in Ref. [2].

In the following, we include explicit expressions for the $\tilde{\chi}_2^\pm$ decays. The corresponding expressions for the $\tilde{\chi}_2^\pm$ decays can be obtained from the given expressions by taking the complex conjugates of the Lorentz-invariant pieces (B, C, D, \dots), with the exception of keeping the propagator functions D_{ij} and \tilde{D} unchanged. As an example, this procedure is demonstrated explicitly for the case of $\tilde{\chi}_2 \rightarrow \tilde{\chi}_1 H_1 H_1$.

1. $X, Y = H_1 H_1$

The amplitude for $\tilde{\chi}_2^- \rightarrow \tilde{\chi}_1^- H_1 H_1$ is given by

$$\begin{aligned} \mathcal{M}^{H_1 H_1} = & \bar{u}_{\tilde{\chi}_1}(s_2, p_2)[(B + C\gamma^5) + \not{\xi}(D + F\gamma^5) \\ & + \not{p}(G + H\gamma^5)]u_{\tilde{\chi}_2}(s_1, p_1), \end{aligned} \quad (\text{A3})$$

⁴There has been some discussion in the literature regarding the correct form to use for the propagator of a spin-1 particle when the particle’s width contributes to a rate asymmetry. See, for example, Ref. [37]. While this discussion is important in some contexts, we nevertheless use the “naive” form of the Z propagator in our numerical work, since the intermediate Z boson is far off shell in the examples we consider.

where $\rho^\mu = (p_2 + p_3)^\mu$, $\xi^\mu = (p_2 + p_4)^\mu$ and

$$B = \frac{g\nu}{\sqrt{2}} \sum_{i,j=1}^3 g_{H_i\tilde{\chi}_1^+\tilde{\chi}_2^-}^S D_{ij}(M^2) g_{H_j H_1 H_1} \eta_j - \frac{g^2}{2} \times \sum_{k=1}^2 \eta_{SP,k}^{(-)} m_{\tilde{\chi}_k} [\tilde{D}(\xi^2, m_{\tilde{\chi}_k}^2, \Gamma_{\tilde{\chi}_k}) + \tilde{D}(\rho^2, m_{\tilde{\chi}_k}^2, \Gamma_{\tilde{\chi}_k})], \quad (\text{A4})$$

$$C = \frac{ig\nu}{\sqrt{2}} \sum_{i,j=1}^3 g_{H_i\tilde{\chi}_1^+\tilde{\chi}_2^-}^P D_{ij}(M^2) g_{H_j H_1 H_1} \eta_j - \frac{ig^2}{2} \times \sum_{k=1}^2 \eta_{PS,k}^{(+)} m_{\tilde{\chi}_k} [\tilde{D}(\xi^2, m_{\tilde{\chi}_k}^2, \Gamma_{\tilde{\chi}_k}) + \tilde{D}(\rho^2, m_{\tilde{\chi}_k}^2, \Gamma_{\tilde{\chi}_k})], \quad (\text{A5})$$

$$\begin{aligned} D &= -\frac{g^2}{2} \sum_{k=1}^2 \eta_{SP,k}^{(+)} \tilde{D}(\xi^2, m_{\tilde{\chi}_k}^2, \Gamma_{\tilde{\chi}_k}), \\ F &= -\frac{ig^2}{2} \sum_{k=1}^2 \eta_{PS,k}^{(-)} \tilde{D}(\xi^2, m_{\tilde{\chi}_k}^2, \Gamma_{\tilde{\chi}_k}), \\ G &= -\frac{g^2}{2} \sum_{k=1}^2 \eta_{SP,k}^{(+)} \tilde{D}(\rho^2, m_{\tilde{\chi}_k}^2, \Gamma_{\tilde{\chi}_k}), \\ H &= -\frac{ig^2}{2} \sum_{k=1}^2 \eta_{PS,k}^{(-)} \tilde{D}(\rho^2, m_{\tilde{\chi}_k}^2, \Gamma_{\tilde{\chi}_k}), \end{aligned} \quad (\text{A6})$$

where we have defined $M^2 = (p_3 + p_4)^2$, $\eta_{\alpha\beta,k}^{(\pm)} = g_{H_1\tilde{\chi}_1^+\tilde{\chi}_k^-}^S g_{H_1\tilde{\chi}_k^+\tilde{\chi}_2^-}^\alpha \pm g_{H_1\tilde{\chi}_1^+\tilde{\chi}_k^-}^P g_{H_1\tilde{\chi}_k^+\tilde{\chi}_2^-}^\beta$, and the factors η_j are $\eta_1 = 6$ and $\eta_{2,3} = 2$. Also, the $m_{\tilde{\chi}_k}$ denote the chargino masses.

The amplitude for $\tilde{\chi}_2^+ \rightarrow \tilde{\chi}_1^+ H_1 H_1$ is given by

$$\begin{aligned} \bar{\mathcal{M}}^{H_1 H_1} &= \bar{u}_{\tilde{\chi}_1}(s_2, p_2) [(\bar{B} + \bar{C}\gamma^5) + \not{\xi}(\bar{D} + \bar{F}\gamma^5) \\ &\quad + \not{p}(\bar{G} + \bar{H}\gamma^5)] u_{\tilde{\chi}_2}(s_1, p_1), \end{aligned} \quad (\text{A7})$$

where

$$\begin{aligned} \bar{B} &= \frac{g\nu}{\sqrt{2}} \sum_{i,j=1}^3 g_{H_i\tilde{\chi}_1^+\tilde{\chi}_2^-}^{S*} D_{ij}(M^2) g_{H_j H_1 H_1} \eta_j - \frac{g^2}{2} \sum_{k=1}^2 \eta_{SP,k}^{(-)*} m_{\tilde{\chi}_k} [\tilde{D}(\xi^2, m_{\tilde{\chi}_k}^2, \Gamma_{\tilde{\chi}_k}) + \tilde{D}(\rho^2, m_{\tilde{\chi}_k}^2, \Gamma_{\tilde{\chi}_k})], \\ \bar{C} &= -\frac{ig\nu}{\sqrt{2}} \sum_{i,j=1}^3 g_{H_i\tilde{\chi}_1^+\tilde{\chi}_2^-}^{P*} D_{ij}(M^2) g_{H_j H_1 H_1} \eta_j + \frac{ig^2}{2} \sum_{k=1}^2 \eta_{PS,k}^{(+)*} m_{\tilde{\chi}_k} [\tilde{D}(\xi^2, m_{\tilde{\chi}_k}^2, \Gamma_{\tilde{\chi}_k}) + \tilde{D}(\rho^2, m_{\tilde{\chi}_k}^2, \Gamma_{\tilde{\chi}_k})], \\ \bar{D} &= -\frac{g^2}{2} \sum_{k=1}^2 \eta_{SP,k}^{(+)*} \tilde{D}(\xi^2, m_{\tilde{\chi}_k}^2, \Gamma_{\tilde{\chi}_k}), \\ \bar{F} &= \frac{ig^2}{2} \sum_{k=1}^2 \eta_{PS,k}^{(-)*} \tilde{D}(\xi^2, m_{\tilde{\chi}_k}^2, \Gamma_{\tilde{\chi}_k}), \\ \bar{G} &= -\frac{g^2}{2} \sum_{k=1}^2 \eta_{SP,k}^{(+)*} \tilde{D}(\rho^2, m_{\tilde{\chi}_k}^2, \Gamma_{\tilde{\chi}_k}), \\ \bar{H} &= \frac{ig^2}{2} \sum_{k=1}^2 \eta_{PS,k}^{(-)*} \tilde{D}(\rho^2, m_{\tilde{\chi}_k}^2, \Gamma_{\tilde{\chi}_k}). \end{aligned} \quad (\text{A8})$$

Note that the spinors $u_{\tilde{\chi}_{1,2}}$ in Eqs. (A3) and (A7) actually refer to $u_{\tilde{\chi}_{1,2}^-}$ in both cases. Here, and throughout this work, we have manipulated expressions in such a way that the $\tilde{\chi}_2^+$ decay amplitudes are written in terms of the spinors $u_{\tilde{\chi}_{1,2}^-}$.

2. $X, Y = ZZ$

The amplitude for $\tilde{\chi}_2^- \rightarrow \tilde{\chi}_1^- ZZ$ is given by

$$\begin{aligned} \mathcal{M}^{ZZ} = & \bar{u}_{\tilde{\chi}_1}(s_2, p_2)[(B + C\gamma^5)g^{\mu\nu} + \gamma^\nu \not{\xi} \gamma^\mu (D + F\gamma^5) \\ & + \gamma^\mu \not{p} \gamma^\nu (G + H\gamma^5) + \gamma^\mu \gamma^\nu (J + K\gamma^5)] \\ & \times u_{\tilde{\chi}_2}(s_1, p_1) \epsilon_\mu^{\lambda_1*} \epsilon_\nu^{\lambda_2*}, \end{aligned} \quad (\text{A9})$$

where

$$\begin{aligned} B = & \frac{g^2 m_W}{\sqrt{2} \cos^2 \theta_W} \sum_{i,j=1}^3 g_{H_i \tilde{\chi}_1^+ \tilde{\chi}_2^-}^S D_{ij}(M^2) g_{H_j V V} \\ & - \frac{g^2}{4 \cos^2 \theta_W} \sum_{k=1}^2 m_{\tilde{\chi}_k} \omega_{RL,k}^+ \tilde{D}(\xi^2, m_{\tilde{\chi}_k}^2, \Gamma_{\tilde{\chi}_k}), \end{aligned} \quad (\text{A10})$$

$$\begin{aligned} C = & \frac{ig^2 m_W}{\sqrt{2} \cos^2 \theta_W} \sum_{i,j=1}^3 g_{H_i \tilde{\chi}_1^+ \tilde{\chi}_2^-}^P D_{ij}(M^2) g_{H_j V V} \\ & - \frac{g^2}{4 \cos^2 \theta_W} \sum_{k=1}^2 m_{\tilde{\chi}_k} \omega_{RL,k}^- \tilde{D}(\xi^2, m_{\tilde{\chi}_k}^2, \Gamma_{\tilde{\chi}_k}), \end{aligned} \quad (\text{A11})$$

$$D = -\frac{g^2}{8 \cos^2 \theta_W} \sum_{k=1}^2 \omega_{LR,k}^+ \tilde{D}(\xi^2, m_{\tilde{\chi}_k}^2, \Gamma_{\tilde{\chi}_k}),$$

$$F = \frac{g^2}{8 \cos^2 \theta_W} \sum_{k=1}^2 \omega_{LR,k}^- \tilde{D}(\xi^2, m_{\tilde{\chi}_k}^2, \Gamma_{\tilde{\chi}_k}),$$

$$G = -\frac{g^2}{8 \cos^2 \theta_W} \sum_{k=1}^2 \omega_{LR,k}^+ \tilde{D}(\rho^2, m_{\tilde{\chi}_k}^2, \Gamma_{\tilde{\chi}_k}),$$

$$H = \frac{g^2}{8 \cos^2 \theta_W} \sum_{k=1}^2 \omega_{LR,k}^- \tilde{D}(\rho^2, m_{\tilde{\chi}_k}^2, \Gamma_{\tilde{\chi}_k}), \quad (\text{A12})$$

$$J = \sum_{k=1}^2 \frac{g^2 m_{\tilde{\chi}_k} \omega_{RL,k}^+}{8 \cos^2 \theta_W} [\tilde{D}(\xi^2, m_{\tilde{\chi}_k}^2, \Gamma_{\tilde{\chi}_k}) - \tilde{D}(\rho^2, m_{\tilde{\chi}_k}^2, \Gamma_{\tilde{\chi}_k})],$$

$$K = \sum_{k=1}^2 \frac{g^2 m_{\tilde{\chi}_k} \omega_{RL,k}^-}{8 \cos^2 \theta_W} [\tilde{D}(\xi^2, m_{\tilde{\chi}_k}^2, \Gamma_{\tilde{\chi}_k}) - \tilde{D}(\rho^2, m_{\tilde{\chi}_k}^2, \Gamma_{\tilde{\chi}_k})],$$

and where we have defined $\omega_{\alpha\beta,k}^{(\pm)} = U_{(L)}^{1k} U_{(\alpha)}^{k2} \pm U_{(R)}^{1k} U_{(\beta)}^{k2}$, with

$$\begin{aligned} U_{(L)}^{ij} &= (C_L)^{i1} (C_L)^{*j1} + (\cos^2 \theta_W - \sin^2 \theta_W) \delta^{ij}, \\ U_{(R)}^{ij} &= (C_R)^{i1} (C_R)^{*j1} + (\cos^2 \theta_W - \sin^2 \theta_W) \delta^{ij}. \end{aligned} \quad (\text{A13})$$

The unitary matrices C_L and C_R are used to diagonalize the chargino mass matrix. The matrices $U_{(L,R)}$ appear in the chargino-chargino- Z Lagrangian as follows,

$$\mathcal{L}_{Z\chi_i\chi_j} = \frac{g}{2 \cos \theta_W} \bar{\chi}_i^- \gamma^\mu [U_{(L)}^{ij} P_L + U_{(R)}^{ij} P_R] \chi_j^- Z_\mu, \quad (\text{A14})$$

where $P_{L(R)} = (1 - (+)\gamma^5)/2$.

3. $X, Y = W^+ W^-$

The amplitude for $\tilde{\chi}_2^- \rightarrow \tilde{\chi}_1^- W^+ W^-$ is given by

$$\begin{aligned} \mathcal{M}^{WW} = & \bar{u}_{\tilde{\chi}_1}(s_2, p_2) \left[(B + C\gamma^5)g^{\mu\nu} + \gamma^\mu \not{p} \gamma^\nu (D + F\gamma^5) \right. \\ & + \gamma^\mu \gamma^\nu (G + H\gamma^5) + \left. \left(\gamma^\nu p_4^\mu - \gamma^\mu p_3^\nu \right. \right. \\ & + \left. \left. \frac{1}{2} (\not{p}_3 - \not{p}_4) g^{\mu\nu} \right) (J + K\gamma^5) \right] \\ & \times u_{\tilde{\chi}_2}(s_1, p_1) \epsilon_\mu^{\lambda_1*} \epsilon_\nu^{\lambda_2*}, \end{aligned} \quad (\text{A15})$$

where p_4 denotes the momentum of the W^- and where

$$\begin{aligned} B = & \frac{g^2 m_W}{\sqrt{2}} \sum_{i,j=1}^3 g_{H_i \tilde{\chi}_1^+ \tilde{\chi}_2^-}^S g_{H_j V V} D_{ij}(M^2), \\ C = & \frac{ig^2 m_W}{\sqrt{2}} \sum_{i,j=1}^3 g_{H_i \tilde{\chi}_1^+ \tilde{\chi}_2^-}^P g_{H_j V V} D_{ij}(M^2), \\ D = & -\frac{g^2}{2} \sum_{k=1}^4 \bar{V}_{LR,k}^+ \tilde{D}(\rho^2, m_{\tilde{\chi}_k}^2, \Gamma_{\tilde{\chi}_k}^0), \\ F = & \frac{g^2}{2} \sum_{k=1}^4 \bar{V}_{LR,k}^- \tilde{D}(\rho^2, m_{\tilde{\chi}_k}^2, \Gamma_{\tilde{\chi}_k}^0), \\ G = & -\frac{g^2}{2} \sum_{k=1}^4 m_{\tilde{\chi}_k} \bar{V}_{RL,k}^+ \tilde{D}(\rho^2, m_{\tilde{\chi}_k}^2, \Gamma_{\tilde{\chi}_k}^0), \\ H = & -\frac{g^2}{2} \sum_{k=1}^4 m_{\tilde{\chi}_k} \bar{V}_{RL,k}^- \tilde{D}(\rho^2, m_{\tilde{\chi}_k}^2, \Gamma_{\tilde{\chi}_k}^0), \\ J = & \frac{g^2}{2} [U_R^{12} + U_L^{12}] \tilde{D}(M^2, m_Z^2, \Gamma_Z), \\ K = & \frac{g^2}{2} [U_R^{12} - U_L^{12}] \tilde{D}(M^2, m_Z^2, \Gamma_Z). \end{aligned} \quad (\text{A16})$$

In the above expressions, $m_{\tilde{\chi}_k}^0$ and $\Gamma_{\tilde{\chi}_k}^0$ denote the neutralino masses and widths, respectively. Also, we define $\bar{V}_{\alpha\beta,k}^\pm$ as $\bar{V}_{\alpha\beta,k}^\pm = V_{(L)}^{k1} V_{(\alpha)}^{k2*} \pm V_{(R)}^{k1} V_{(\beta)}^{k2*}$, where

$$\begin{aligned} V_{(L)}^{ij} &= (N)^{*i2} (C_L)^{j1} + \frac{1}{\sqrt{2}} (N)^{*i3} (C_L)^{j2}, \\ V_{(R)}^{ij} &= (N)^{i2} (C_R)^{j1} - \frac{1}{\sqrt{2}} (N)^{i4} (C_R)^{j2}. \end{aligned}$$

The 4×4 unitary matrix N is used to diagonalize the neutralino mass matrix.

4. $X, Y = ZH_1$

The amplitude for $\tilde{\chi}_2^- \rightarrow \tilde{\chi}_1^- ZH_1$ is given by

$$\begin{aligned} \mathcal{M}^{ZH_1} = & \bar{u}_{\tilde{\chi}_1}(s_2, p_2) [(B + C\gamma^5) p_4^\mu \\ & + (D + F\gamma^5) \gamma^\mu + (G + H\gamma^5) \not{\xi} \gamma^\mu \\ & + (J + K\gamma^5) \gamma^\mu \not{p}] u_{\tilde{\chi}_2}(s_1, p_1) \epsilon_\mu^{\lambda*}, \end{aligned} \quad (\text{A17})$$

where p_4 denotes the momentum of the H_1 in the final state and where

$$\begin{aligned}
B &= -\frac{ig^2}{\sqrt{2}\cos\theta_W} \sum_{i=1,j=2}^3 g_{H_i\tilde{\chi}_1^+\tilde{\chi}_2^-}^S D_{ij}(M^2) g_{H_1H_jZ} - \frac{g^2 m_W}{8\cos^3\theta_W m_Z^2} g_{H_1VV}(m_{\tilde{\chi}_2^-} - m_{\tilde{\chi}_1^+}) [U_L^{12} + U_R^{12}] \tilde{D}(M^2, m_Z^2, \Gamma_Z), \\
C &= \frac{g^2}{\sqrt{2}\cos\theta_W} \sum_{i=1,j=2}^3 g_{H_i\tilde{\chi}_1^+\tilde{\chi}_2^-}^P D_{ij}(M^2) g_{H_1H_jZ} - \frac{g^2 m_W}{8\cos^3\theta_W m_Z^2} g_{H_1VV}(m_{\tilde{\chi}_1^+} + m_{\tilde{\chi}_2^-}) [U_L^{12} - U_R^{12}] \tilde{D}(M^2, m_Z^2, \Gamma_Z), \\
D &= \sum_{k=1}^2 \frac{g^2 m_{\tilde{\chi}_k} \tilde{D}(\rho^2, m_{\tilde{\chi}_k}^2, \Gamma_{\tilde{\chi}_k})}{4\sqrt{2}\cos\theta_W} [U_L^{1k}(g_{H_1\tilde{\chi}_k^+\tilde{\chi}_2^-}^S - ig_{H_1\tilde{\chi}_k^+\tilde{\chi}_2^-}^P) + U_R^{1k}(g_{H_1\tilde{\chi}_k^+\tilde{\chi}_2^-}^S + ig_{H_1\tilde{\chi}_k^+\tilde{\chi}_2^-}^P)] \\
&\quad + \sum_{k=1}^2 \frac{g^2 m_{\tilde{\chi}_k} \tilde{D}(\xi^2, m_{\tilde{\chi}_k}^2, \Gamma_{\tilde{\chi}_k})}{4\sqrt{2}\cos\theta_W} [U_L^{k2}(g_{H_1\tilde{\chi}_1^+\tilde{\chi}_k^-}^S + ig_{H_1\tilde{\chi}_1^+\tilde{\chi}_k^-}^P) + U_R^{k2}(g_{H_1\tilde{\chi}_1^+\tilde{\chi}_k^-}^S - ig_{H_1\tilde{\chi}_1^+\tilde{\chi}_k^-}^P)] \\
&\quad + \frac{g^2 m_W}{8\cos^3\theta_W} g_{H_1VV} [U_L^{12} + U_R^{12}] \tilde{D}(M^2, m_Z^2, \Gamma_Z), \\
F &= \sum_{k=1}^2 \frac{g^2 m_{\tilde{\chi}_k} \tilde{D}(\rho^2, m_{\tilde{\chi}_k}^2, \Gamma_{\tilde{\chi}_k})}{4\sqrt{2}\cos\theta_W} [U_L^{1k}(g_{H_1\tilde{\chi}_k^+\tilde{\chi}_2^-}^S - ig_{H_1\tilde{\chi}_k^+\tilde{\chi}_2^-}^P) - U_R^{1k}(g_{H_1\tilde{\chi}_k^+\tilde{\chi}_2^-}^S + ig_{H_1\tilde{\chi}_k^+\tilde{\chi}_2^-}^P)] \\
&\quad + \sum_{k=1}^2 \frac{g^2 m_{\tilde{\chi}_k} \tilde{D}(\xi^2, m_{\tilde{\chi}_k}^2, \Gamma_{\tilde{\chi}_k})}{4\sqrt{2}\cos\theta_W} [U_L^{k2}(g_{H_1\tilde{\chi}_1^+\tilde{\chi}_k^-}^S + ig_{H_1\tilde{\chi}_1^+\tilde{\chi}_k^-}^P) - U_R^{k2}(g_{H_1\tilde{\chi}_1^+\tilde{\chi}_k^-}^S - ig_{H_1\tilde{\chi}_1^+\tilde{\chi}_k^-}^P)] \\
&\quad + \frac{g^2 m_W}{8\cos^3\theta_W} g_{H_1VV} [U_L^{12} - U_R^{12}] \tilde{D}(M^2, m_Z^2, \Gamma_Z), \\
G &= \sum_{k=1}^2 \frac{g^2 \tilde{D}(\xi^2, m_{\tilde{\chi}_k}^2, \Gamma_{\tilde{\chi}_k})}{4\sqrt{2}\cos\theta_W} [U_L^{k2}(g_{H_1\tilde{\chi}_1^+\tilde{\chi}_k^-}^S - ig_{H_1\tilde{\chi}_1^+\tilde{\chi}_k^-}^P) + U_R^{k2}(g_{H_1\tilde{\chi}_1^+\tilde{\chi}_k^-}^S + ig_{H_1\tilde{\chi}_1^+\tilde{\chi}_k^-}^P)], \\
H &= \sum_{k=1}^2 \frac{g^2 \tilde{D}(\xi^2, m_{\tilde{\chi}_k}^2, \Gamma_{\tilde{\chi}_k})}{4\sqrt{2}\cos\theta_W} [-U_L^{k2}(g_{H_1\tilde{\chi}_1^+\tilde{\chi}_k^-}^S - ig_{H_1\tilde{\chi}_1^+\tilde{\chi}_k^-}^P) + U_R^{k2}(g_{H_1\tilde{\chi}_1^+\tilde{\chi}_k^-}^S + ig_{H_1\tilde{\chi}_1^+\tilde{\chi}_k^-}^P)], \\
J &= \sum_{k=1}^2 \frac{g^2 \tilde{D}(\rho^2, m_{\tilde{\chi}_k}^2, \Gamma_{\tilde{\chi}_k})}{4\sqrt{2}\cos\theta_W} [U_L^{1k}(g_{H_1\tilde{\chi}_k^+\tilde{\chi}_2^-}^S + ig_{H_1\tilde{\chi}_k^+\tilde{\chi}_2^-}^P) + U_R^{1k}(g_{H_1\tilde{\chi}_k^+\tilde{\chi}_2^-}^S - ig_{H_1\tilde{\chi}_k^+\tilde{\chi}_2^-}^P)], \\
K &= \sum_{k=1}^2 \frac{g^2 \tilde{D}(\rho^2, m_{\tilde{\chi}_k}^2, \Gamma_{\tilde{\chi}_k})}{4\sqrt{2}\cos\theta_W} [U_L^{1k}(g_{H_1\tilde{\chi}_k^+\tilde{\chi}_2^-}^S + ig_{H_1\tilde{\chi}_k^+\tilde{\chi}_2^-}^P) - U_R^{1k}(g_{H_1\tilde{\chi}_k^+\tilde{\chi}_2^-}^S - ig_{H_1\tilde{\chi}_k^+\tilde{\chi}_2^-}^P)].
\end{aligned} \tag{A18}$$

As noted above, our notation for $g_{H_iH_jZ}$ is the same as that adopted in Ref. [2].

-
- | | |
|---|---|
| [1] K. Kiers, A. Szykman, and D. London, Phys. Rev. D 74 , 035004 (2006). | [8] P. Osland and A. Vereshagin, Phys. Rev. D 76 , 036001 (2007). |
| [2] A. Szykman, K. Kiers, and D. London, Phys. Rev. D 75 , 075009 (2007). | [9] K. Rolbieceki and J. Kalinowski, Phys. Rev. D 76 , 115006 (2007). |
| [3] W.M. Yang and D.S. Du, Phys. Rev. D 67 , 055004 (2003). | [10] A. Bartl, K. Hohenwarter-Sodek, T. Kernreiter, O. Kittel, and M. Terwort, Nucl. Phys. B802 , 77 (2008). |
| [4] A. Bartl, H. Fraas, O. Kittel, and W. Majerotto, Phys. Lett. B 598 , 76 (2004). | [11] O. Kittel and F. von der Pahlen, J. High Energy Phys. 08 (2008) 030. |
| [5] O. Kittel, A. Bartl, H. Fraas, and W. Majerotto, Phys. Rev. D 70 , 115005 (2004). | [12] F. Gabbiani and A. Masiero, Nucl. Phys. B322 , 235 (1989); S. Bertolini, F. Borzumati, A. Masiero, and G. Ridolfi, Nucl. Phys. B353 , 591 (1991); J. S. Hagelin, S. Kelley, and T. Tanaka, Nucl. Phys. B415 , 293 (1994). |
| [6] H. Eberl, T. Gajdosik, W. Majerotto, and B. Schrausser, Phys. Lett. B 618 , 171 (2005). | [13] A. Ali and D. London, Eur. Phys. J. C 9 , 687 (1999). |
| [7] A. Bartl, H. Fraas, S. Hesselbach, K. Hohenwarter-Sodek, T. Kernreiter, and G. Moortgat-Pick, Eur. Phys. J. C 51 , 149 (2007). | [14] F. Gabbiani, E. Gabrielli, A. Masiero, and L. Silvestrini, Nucl. Phys. B477 , 321 (1996); Y. Grossman, Y. Nir, and R. |

- Rattazzi, *Adv. Ser. Dir. High Energy Phys.* **15**, 755 (1998); D. Chang, W.-Y. Keung, and A. Pilaftsis, *Phys. Rev. Lett.* **82**, 900 (1999); A. Pilaftsis and C.E.M. Wagner, *Nucl. Phys.* **B553**, 3 (1999); S. Abel, S. Khalil, and O. Lebedev, *Nucl. Phys.* **B606**, 151 (2001); D. A. Demir, O. Lebedev, K. A. Olive, M. Pospelov, and A. Ritz, *Nucl. Phys.* **B680**, 339 (2004); K. A. Olive, M. Pospelov, A. Ritz, and Y. Santoso, *Phys. Rev. D* **72**, 075001 (2005).
- [15] J. S. Lee, A. Pilaftsis, M. Carena, S. Y. Choi, M. Drees, J. R. Ellis, and C. E. M. Wagner, *Comput. Phys. Commun.* **156**, 283 (2004).
- [16] J. S. Lee, M. Carena, J. Ellis, A. Pilaftsis, and C. E. M. Wagner, *Comput. Phys. Commun.* **180**, 312 (2009).
- [17] J. R. Ellis, J. S. Lee, and A. Pilaftsis, *J. High Energy Phys.* **10** (2008) 049.
- [18] J. R. Ellis, J. S. Lee, and A. Pilaftsis, *Phys. Rev. D* **70**, 075010 (2004).
- [19] See, for example, J. F. Gunion, H. E. Haber, G. L. Kane, and S. Dawson, *The Higgs Hunter's Guide* (Addison-Wesley, Reading, MA, 1990); H. E. Haber, arXiv:hep-ph/9707213.
- [20] J. Rosiek, *Phys. Rev. D* **41**, 3464 (1990).
- [21] J. Rosiek, arXiv:hep-ph/9511250.
- [22] R. Mertig, M. Bohm, and A. Denner, *Comput. Phys. Commun.* **64**, 345 (1991).
- [23] J. M. Gerard and W. S. Hou, *Phys. Rev. Lett.* **62**, 855 (1989).
- [24] L. Wolfenstein, *Phys. Rev. D* **43**, 151 (1991).
- [25] K. Philippides and A. Sirlin, *Phys. Lett. B* **367**, 377 (1996).
- [26] J. Papavassiliou and A. Pilaftsis, *Phys. Rev. D* **53**, 2128 (1996).
- [27] M. S. Carena, J. R. Ellis, A. Pilaftsis, and C. E. M. Wagner, *Phys. Lett. B* **495**, 155 (2000).
- [28] J. S. M. Ginges and V. V. Flambaum, *Phys. Rep.* **397**, 63 (2004).
- [29] B. C. Regan, E. D. Commins, C. J. Schmidt, and D. DeMille, *Phys. Rev. Lett.* **88**, 071805 (2002).
- [30] W. C. Griffith, M. D. Swallows, T. H. Loftus, M. V. Romalis, B. R. Heckel, and E. N. Fortson, *Phys. Rev. Lett.* **102**, 101601 (2009).
- [31] C. A. Baker *et al.*, *Phys. Rev. Lett.* **97**, 131801 (2006).
- [32] G. W. Bennett *et al.* (Muon (g-2) Collaboration), *Phys. Rev. D* **80**, 052008 (2009).
- [33] K. Cheung, O. C. W. Kong, and J. S. Lee, *J. High Energy Phys.* **06** (2009) 020.
- [34] Heavy Flavor Averaging Group, <http://www.slac.stanford.edu/xorg/hfag>.
- [35] C. Amsler *et al.* (Particle Data Group), *Phys. Lett. B* **667**, 1 (2008) and 2009 partial update for the 2010 edition, <http://pdg.lbl.gov>.
- [36] J. R. Ellis, J. S. Lee, and A. Pilaftsis, *Phys. Rev. D* **76**, 115011 (2007).
- [37] D. Atwood, G. Eilam, A. Soni, R. R. Mendel, and R. Migneron, *Phys. Rev. D* **49**, 289 (1994).